Analysis of the Contribution of the Microfibrils and Matrix to the Deformation Processes in Wool Fibers

Katherina Tsobkallo,[1] Baki Aksakal,[2] Diana Darvish[1]

[1]*Department of Mechanics of Materials, St. Petersburg State University of Technology and Design, B. Morskaya 18, St. Petersburg 191186, Russia*
[2]*Department of Physics, Davutpasa Campus, Yildiz Technical University, Esenler 34210, Istanbul, Turkey*

Received 6 April 2011; accepted 23 November 2011
DOI 10.1002/app.36535
Published online in Wiley Online Library (wileyonlinelibrary.com).

ABSTRACT: In this study, the mechanical and structural characteristics of wool fibers were examined, and the contributions of the microfibrils and matrix to the deformation processes were analyzed. The experiments were carried out on single wool fibers. To understand the structural changes at different deformation levels, the wool fibers were treated with a complex mechanical regime. One of the most significant results from the mechanical tests was the estimation of the modulus of the matrix, which changed from 0.07 to 1.6 GPa during stretching. This result proves the proposal of the netlike structure of the matrix. On the basis of the obtained experimental data and the structural model, where the microfibrils and matrix play the role of a reinforcing phase and a filler, respectively, the rigidity of the microfibrils in the initial unstretched state was determined to be equal to about 20 GPa. The experimental data obtained from the Fourier transform infrared–attenuated total reflectance spectroscopy method proved the α–β conformational transition both in the yield and postyield regions and revealed the presence of the stable β form, which was not sensitive to stretching. © 2012 Wiley Periodicals, Inc. J Appl Polym Sci 000: 000–000, 2012

Key words: matrix; mechanical properties; structure–property relations

INTRODUCTION

Wool fibers from the family of α-keratin fibers have a very complex multilayer structure. According to some authors,[1–3] the most important structural units that determine its mechanical properties are the microfibrils and the matrix. Microfibrils represent the crystalline part in the fiber structure, and they are surrounded by an amorphous matrix phase.[4] Polypeptide macromolecules in microfibrils have a predominantly α-helical conformation; however, some authors have stated that there is about a 40% β-sheet content.[5,6] These are held together by intermolecular and intramolecular interactions such as hydrogen bonds, van der Waals interactions, some salt linkages and disulfide bonds (crosslinks).[1,7,8] The amorphous matrix consists of matrix globules connected to each other and with microfibrils by disulfide crosslinks and also different kinds of intermolecular interactions.[9] Such structural organization of the α-keratin fibers determines wool's unique mechanical behavior.

There have been lots of studies dedicated to the examination of the mechanical behavior of α-keratin fibers; they have mainly been done on wool fibers,[1–3,10] where the elongation process of the fiber is commonly divided into three distinct regions: the Hookean region from 0 to 2% strain, the yield region from 2 to 25–30% strain, and the postyield region beyond 30% strain. The interpretation of the structural processes in these three deformation regions has been introduced by several authors, and some structural models have been proposed.[2–4,10,11]

The first structural model, the so-called two-phase model, was proposed by Feughelman in 1959.[4] He described the mechanical behavior of α-keratin fiber by regarding two main phases in the structure: non-water-absorbing microfibrils (phase C) embedded into a water-absorbing matrix (phase M). In this model, the initial Hookean deformation is attributed to the changes in bond angles and bond spacing, and the yield region is attributed to the conformational transition of the macromolecules in microfibrils from α helices to the extended β sheets. However, this model cannot explain the increase in stiffness in the postyield region. Later, Feughelman and Haly[12] proposed a new series-zone model in which microfibrils are regarded to be composed of alternating *X* and *Y* zones with different rigidities. It was stated that *X* zones undergo the α–β transition in the yield region and the stiffer *Y* zones do so in the postyield region.

Another model was proposed by Hearle[2] and Chapman,[10] where it was assumed that the microfibrils are connected mechanically to the matrix via a

Correspondence to: B. Aksakal (aksakal@yildiz.edu.tr).

number of covalent linkages situated at intervals along the length of the microfibrils. It was also suggested that in the yield region, microfibrils undergo an α–β transition in parallel with the elongation of the elastomeric amorphous matrix. The postyield region is associated with the increasing rigidity of the matrix during stretching. Moreover, in this model, independent stress–strain curves of the microfibrils and the matrix are suggested.

Two new models appeared in 1994, one of which was proposed by Feughelman[9] and another one by Wortmann and Zahn.[3] Fughelman, in his new model, considered the matrix to be globular proteins surrounded by water molecules. Here, the change from the yield to postyield region is attributed to the jamming of the globules between microfibrils during extension.

Wortmann and Zahn[3] presented a more detailed series-zone model. It is based on a well-established knowledge of the detailed structure of microfibrils. This model attributes all of the mechanical behaviors of the fiber to the properties of the microfibrils and neglects the role of the matrix.

Obviously, the presented structural models, which interpret the structural–mechanical properties relationship of α-keratin fibers,[3,4,9–12] still have some controversies, which can only be solved by a new set of experimental data.

Therefore, in this study, we aimed to set the structural–mechanical properties relationship of stretched wool fibers to analyze the contribution of the microfibrils and the matrix to the deformation processes of the wool fibers.

EXPERIMENTAL

Materials

For the experiments, two different sheep wools, namely, white and black originating from Turkey, were chosen. All of the mechanical experiments were carried out on single wool fibers, which were carefully selected by thickness. The diameter of each fiber was determined by measurements at approximately 10 different parts along the fiber with a digital micrometer (Tronic Ip54, Zhejiang, China, 0–25 mm with a sensitivity of 0.001 mm); these measurements were averaged. Only fibers with close values of average diameter were used in the mechanical experiments. The average diameters of the tested fibers were 50 ± 2 μm for the black wool and 70 ± 3 μm for the white wool.

Methods

Mechanical measurements

The mechanical properties of the wool fibers were investigated on a tensile tester (Instron 1122, Buckinghamshire, England). The gauge length of the tested single wool fibers was chosen to be 50 mm. Before measurement, the test fiber was stuck carefully in a paper frame with glue (Pritt, Düsseldorf, Germany). The stress–strain curves of the samples were obtained at a constant strain rate of 100%/min (50 mm/min) at 25°C and a relative humidity of 60%.

To investigate the changes in the mechanical properties of the wool fibers after stretching, the complex regime, including four steps, were realized. The model of this complex regime is shown in Figure 1. The first step (I) was the stretching up to an adjusted deformation level (ε_p). The second step (II) was the relaxation process, which lasted for 10 min at this ε_p. The third step (III) was the subsequent recovery process, which lasted for 10 min. In the last step (IV), the stress–strain curve of this stretched wool fiber was recorded.

Thus, the stress–strain curves of the wool fibers stretched at a wide extension range from 1 to 34% were obtained, and their mechanical characteristics were investigated.

Spectroscopic measurements

Infrared experiments were carried out on a PerkinElmer Fourier Spectrometer Spectrum One, PerkinElmer, Inc., California, USA. The infrared spectra of the samples were recorded with an attenuated total reflectance (ATR) cell. The ATR method allows one to obtain the spectra of fibers without any mechanical destruction, as needed in this study. To investigate the structural changes after stretching, the bunches of wool fibers were stretched in the tensile tester up to different ε_p's, which ranged from 10 to 35% strain, and were then stuck in the rectangular frames and fixed with a strong glue (Pattex Super Glue, Henkel). The Fourier transform infrared (FTIR)–ATR spectra of these stretched samples, which consisted of 30 ± 5 single wool fibers, were recorded in the 550–4000-cm^{-1} range at a resolution of 4 cm^{-1} with four scans for each measurement.

For analysis of the conformational changes and hydrogen bond interactions in the stretched wool fibers, the components of complex amide I, amide III bands, and the wide peak observed at approximately 2400–3800 cm^{-1} were separated by a curve-fitting procedure.

Before curve fitting, the transmission (T; %) spectrum for each spectral region was converted to an absorptance ($100 - T$) versus wave number curve. An appropriate baseline was drawn for each region and then subtracted from the curve. Then, the curve-fitting procedures were applied to these curves with a Gaussian approach. The flat baselines were drawn from 1560 ± 10 to 1750 ± 10, 1100 ± 8 to 1350 ± 3, and 2365 ± 2 to 3955 ± 10 cm^{-1} for the amide I, amide III, and 2350–4000-cm^{-1} regions, respectively.

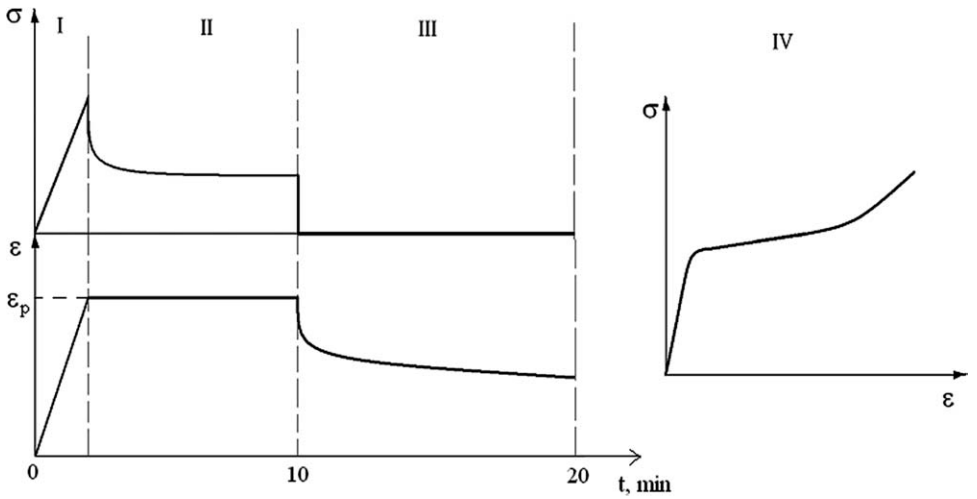

Figure 1 Model showing the complex regime of the stretching of the wool fibers: (I) stretching up to an adjusted ε_p at the constant rate, (II) stress relaxation at a constant ε_p, (III) elastic recovery process, and (IV) stress–strain curve of the stretched fiber (t = time; σ = stress; ε = strain).

By means of the Beer–Lambert law, the absorbance (optical density) calculations, that is, the ratio of absorbance of each component band to that of an internal standard band, were carried out with an internal standard band observed at 1448 cm^{-1} and assigned to the CH_2-scissoring mode.[13,14]

RESULTS AND DISCUSSION

Mechanical properties of the stretched wool fibers

The stress–strain curves of the white and black wool fibers stretched at different ε_p's up to 34% were recorded, and as examples, some of them are shown in Figure 2. As shown, both types of wool fibers showed a similar tendency of the stress–strain curves to change. The stretching of the wool fibers in the first deformation region, that is, $0 < \varepsilon_p \leq 4\%$, did not lead to changes in the mechanical characteristics. Deformation beyond 4% led to considerable changes, depending on ε_p. To analyze the obtained stress–strain curves, the following mechanical characteristics were determined: stress at rupture (σ_r), strain at rupture (ε_r), initial modulus (E_i), and average value of the tangent modulus in the yield region (E_y). Here, E_y was calculated from the slope of the second deformation region (the yield region on the original curve).

The stretching of the wool fibers also caused a decrease in the diameter of the fiber cross section. The dependence of the decrease in the diameter of the cross section on ε_p is shown in Figure 3. It

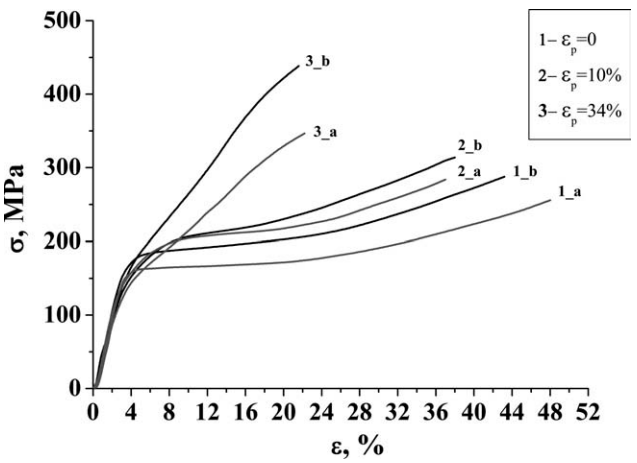

Figure 2 Stress–strain curves of (a) stretched white wool and (b) black wool fibers at different ε_p's (σ = stress; ε = strain).

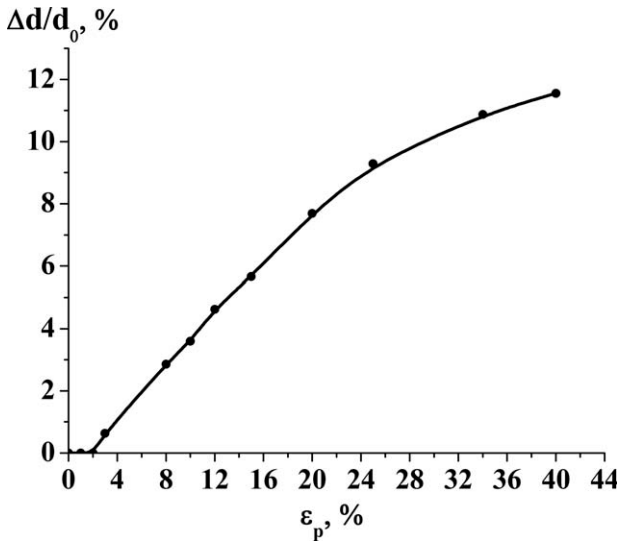

Figure 3 Percentage decrease in the diameter of the wool fibers versus ε_p. Δd is the absolute change in the diameter of the wool fiber and d_0 is the diameter of the unstretched wool fiber.

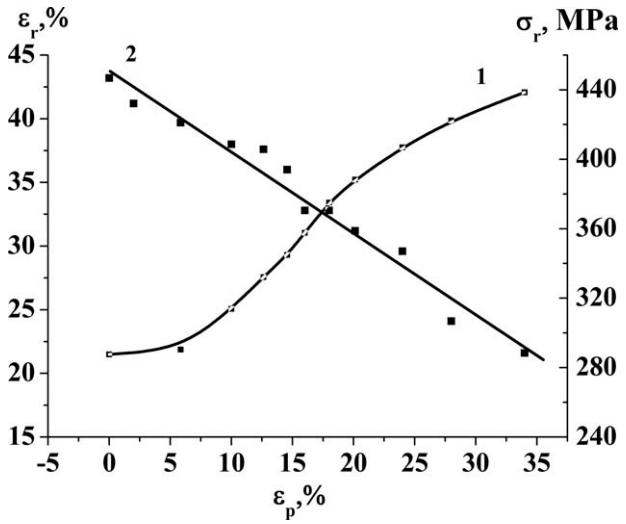

Figure 4 (1) Tensile strength and (2) breaking extension of the black wool fibers versus ε_p.

was obvious that the stretching of the wool fibers at ε_p's lower than 4% did not cause any change in the cross section, whereas deformation in the region of $4\% < \varepsilon_p \leq 24\%$ led to an almost linear decrease in the diameter. At $\varepsilon_p = 28\%$, the decrease in the diameter was about 10%, and stretching at a higher value of ε_p did not bring many changes; for example, the diameter of the fibers stretched at $\varepsilon_p = 35\%$ decreased by around 11–12%.

The change in the breaking characteristics is shown in Figure 4. With increasing ε_p, σ_r also increased, from 290 to 440 MPa, whereas ε_r decreased almost linearly from 45 to 20% strain. The relationship between E_i and ε_p showed that E_i did not depend on the adjusted ε_p and became around 6.5 GPa. This result drew our attention because, for many polymers, extension leads to an increase in the initial rigidity due to orientation processes.[15–17] Another interesting result, as shown in Figure 5,

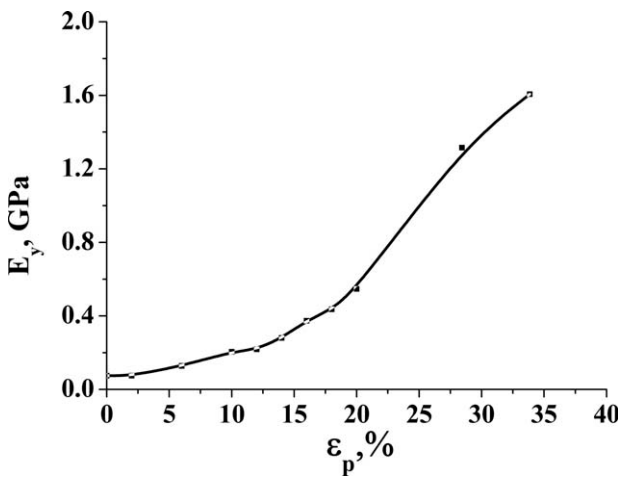

Figure 5 Relationship between the average value of the modulus in the yield region and ε_p.

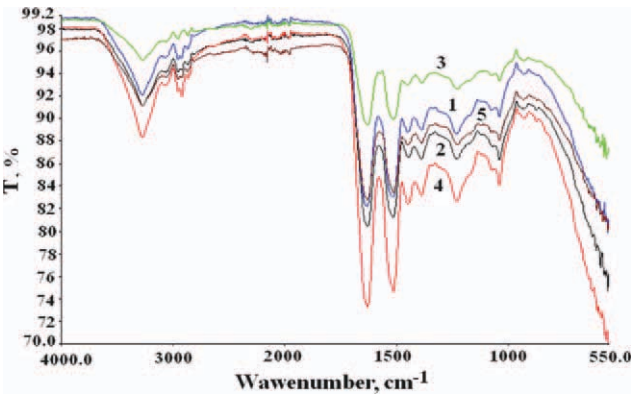

Figure 6 FTIR–ATR spectra of the wool fibers at different ε_p values: (1) 0, (2) 10, (3) 20, (4) 25, and (5) 35%. [Color figure can be viewed in the online issue, which is available at www.interscience.wiley.com.]

was the increase of the average value of E_y in the second deformation region after the application of preliminary stretching. Although ε_p increased up to about 16%, E_y increased slightly, but beyond this value, it increased sharply.

To explain the observed changes in the mechanical characteristics, we analyzed the conformational changes in the fiber structure by using the FTIR–ATR spectroscopy method.

Estimation of the conformational changes in the stretched wool fibers by the FTIR–ATR method

In Figure 6, the infrared spectra of wool fibers stretched at 10, 20, 25, and 35% strain are shown. It is well known that all amide bands were sensitive to conformational changes in the macromolecules; therefore, to estimate the α–β conformational changes in the stretched wool fibers, the amide I and amide III bands were examined carefully.

To analyze the amide I complex band, we accepted that the band with a maximum at 1651 cm^{-1} [5,6,13,18–23] represented the vibration of the α helix, the band with a maximum at 1677 cm^{-1} [5,6,13,19,20] represented the β-sheet structure, and the band at 1624 cm^{-1} was due to the β-sheet parallel.[18] Also, the band component observed at 1695 cm^{-1} was assigned to the amide group of the asparagine and glutamine side chains.[13,22]

In Figure 7, the separation of the amide I band into component bands is shown. The band frequency and half-band width of each component are given in Table I. For the quantitative estimation of conformational changes, the absorbance (D) of each band was divided by that of the standard band. The changes of the absorbency ratios of the concerned peaks with increasing ε_p are shown in Figure 8. Consequently, it is shown that as ε_p increased, the content of α-helical conformation decreased, whereas the content of

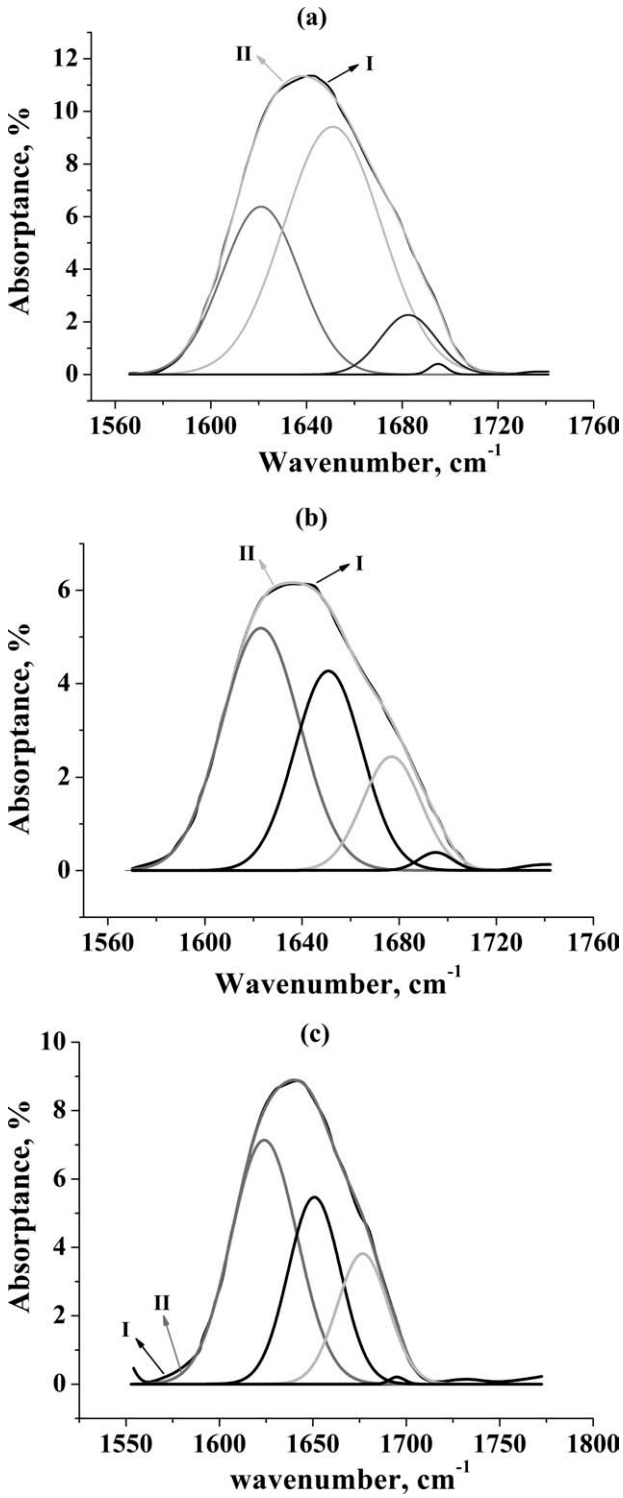

Figure 7 FTIR spectra of the amide I region of the wool fibers extended at different ε_p values: (a) 0, (b) 20, and (c) 35% resolved into components: (I) experimental spectrum and (II) curve fit.

β-sheet conformation increased. However, the content of the β-sheet parallel did not change with increasing ε_p.

Similarly, the amide III region was separated into several bands with curve fitting. The band frequency and half-band width of each component are given in Table II. In the amide III region, the ν(CN) stretching and δ(NH) bending mode,[13,19,20] which are significant components of the α-helical structure, were observed between 1260 and 1300 cm^{-1} with low intensity. Another peak observed at 1230–1240 cm^{-1} was attributed to the mode of the amide group in the β-pleated-sheet structure.[13,19,20] The other two band components observed around 1161 and 1177–1185 cm^{-1} were attributed to the ν(CC)/δ(COH) and ν(CC) modes.[14,19,20] The bands at 1207–1210 and 1301–1318 cm^{-1} were assigned to ν(CC)/tyrosine–phenylalanine and δ(CH_2), respectively.[19,20,24] Figure 9 shows the component bands of the amide III region. Here, to estimate the conformational changes during stretching, just two bands at 1285 and 1230 cm^{-1} were analyzed carefully. Thus, from the analysis of the complex amide III region, it was shown that the ratio of the absorbance of the band at 1285 cm^{-1} to that of standard band decreased, as shown in Figure 10(a). Hence, the number of macromolecules having the α conformation also decreased; this proves the occurrence of a conformational α–β transition during stretching. However, the ratio of the absorbance of the band at 1230 cm^{-1}, which reflected the β conformation[13,19,20] with respect to that of the standard band did not change after stretching, as shown in Figure 10(b). Thus, in the amide III region, we also observed the stable β form, which did not change during stretching.

Hence, the experimental data obtained from the FTIR spectra of the stretched wool fibers at different

TABLE I
Band Frequency and Half-Band Width of the Components in the Amide I Band Region of the FTIR Spectra of Wool Fibers Extended at Different Strain Levels

ε_p (%)	Band frequency (cm^{-1})	Half-band width (cm^{-1})
0	1621	32
	1651	40
	1683	23
	1695	7
10	1623	32
	1651	28
	1677	23
	1695	10
20	1623	32
	1651	28
	1677	23
	1695	14
25	1624	33
	1651	27
	1677	27
	1695	7
35	1624	35
	1651	28
	1677	27
	1695	7

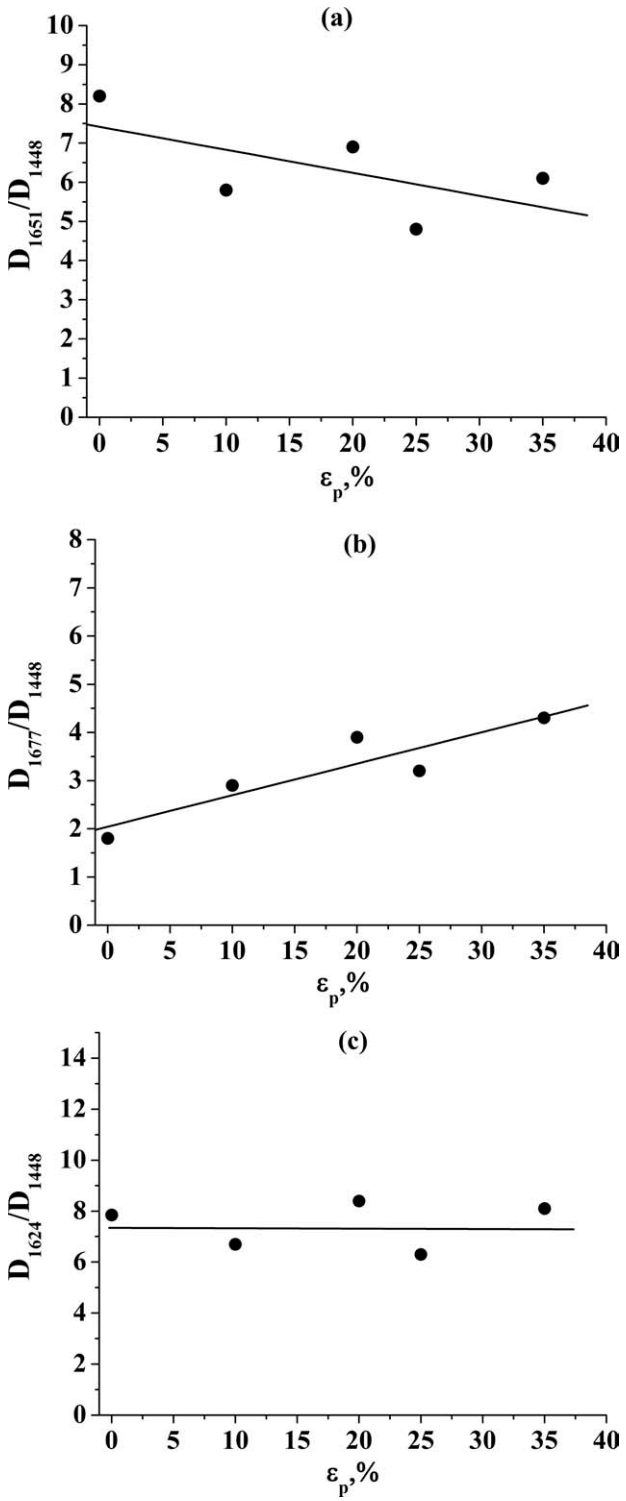

Figure 8 Change in the ratio of the absorbance of the bands at (a) 1651, (b) 1677, and 1624 cm^{-1} to that of the standard band during stretching.

strain levels proved the α–β transition in the α-keratin macromolecules. Also, we noticed that such a conformational transition occurred in both the yield and postyield regions. However, the most interesting experimental result was the presence of the stable β conformation in the α-keratin fiber, which did not change under stretching and did not appear as a consequence of the α–β transition. Such a stable β conformation was characterized by the bands with maxima near 1624 cm^{-1} in the amide I region and 1230 cm^{-1} in the amide III region.

To understand the changes in the water content and hydrogen interactions during stretching, the 2350–4000-cm^{-1} region of the spectra of the stretched wool fibers was examined carefully after the component peaks were separated, as shown in Figure 11. The band frequency and half-band width of each component are given in Table III. In this region, the band above 3500 cm^{-1} was assigned to the O—H band;[25] for instance, symmetric frequency of OH stretching for water was 3651 cm^{-1}.[26] Similarly, in another study, the band around 3500 cm^{-1} was assigned to the OH stretching of free water.[27] Therefore, we assigned the frequency around 3500 cm^{-1} to the OH stretching of free water in the structure. Another band around 3200 cm^{-1} corresponded to the absorbed water in the amorphous phase in keratins.[28,29] The intense band observed around 3280 cm^{-1} was attributed to the NH stretching of hydrogen-bonded NH groups.[27,30,31] The other band observed at

TABLE II
Band Frequency and Half-Band Width of the Components in the Amide III Band Region of the FTIR Spectra of the Wool Fibers Extended at Different Strain Levels

ε_p (%)	Band frequency (cm^{-1})	Half-band width (cm^{-1})
0	1162	21
	1184	26
	1200	12
	1230	45
	1286	35
	1311	11
10	1163	24
	1187	26
	1200	12
	1230	42
	1286	36
	1311	11
20	1160	23
	1182	51
	1198	10
	1231	40
	1283	38
	1311	11
25	1160	20
	1181	39
	1198	11
	1230	42
	1282	43
	1311	11
35	1152	8
	1171	32
	1195	15
	1228	43
	1284	37
	1311	11

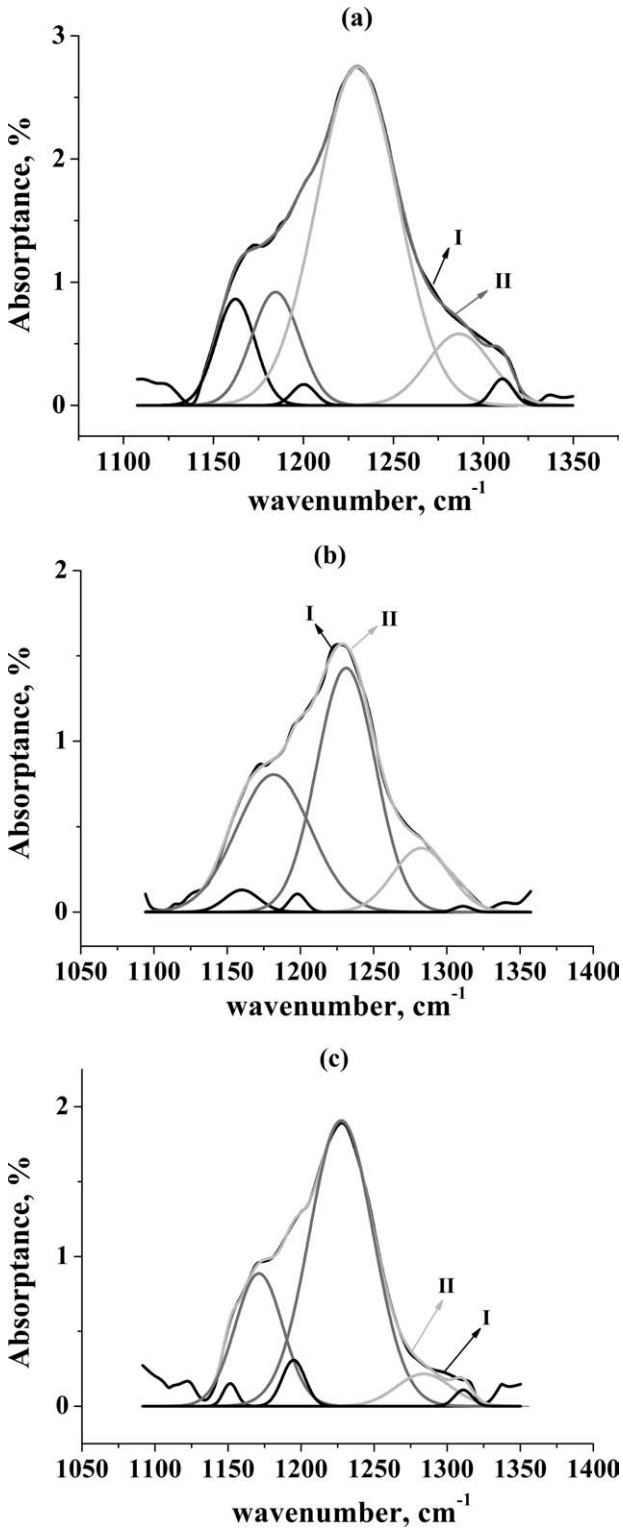

Figure 9 FTIR spectra of the amide III region of the wool fibers extended at different ε_p values: (a) 0, (b) 20, and (c) 35% resolved into components: (I) experimental spectrum and (II) curve fit.

approximately 3400 cm^{-1} was attributed to the vibration of free NH groups.[27,31] The bands observed at approximately 2933 and 3065 cm^{-1} were attributed to the methyl (CH_3) symmetric mode[19,20] the amide B band, which was connected with the frequency of stretching vibrations of located ν(N—H) bonds,[32] respectively.

To analyze the change in the water content and hydrogen-bond interactions, the ratios of the absorbencies of the bands at 3500 and 3280 cm^{-1} to that of the standard band were calculated (Fig. 12). It was revealed that the free water content decreased during stretching because the ratio of the absorbance of the corresponding peak decreased. At the same time, the absorbance of the peak corresponding to the amount of hydrogen-bond interactions did not change significantly. This result was not obvious because the stretching of the wool fiber caused the disruption of hydrogen bonds between successive turns in the helices. Thus, we supposed that during stretching, the reorganization of the hydrogen-bond network occurred: the disruptions of one type of hydrogen-bond interactions caused the appearance of new ones. Consequently, from our experimental results, we observed that the stretching of the wool fibers led to the removal of the some water

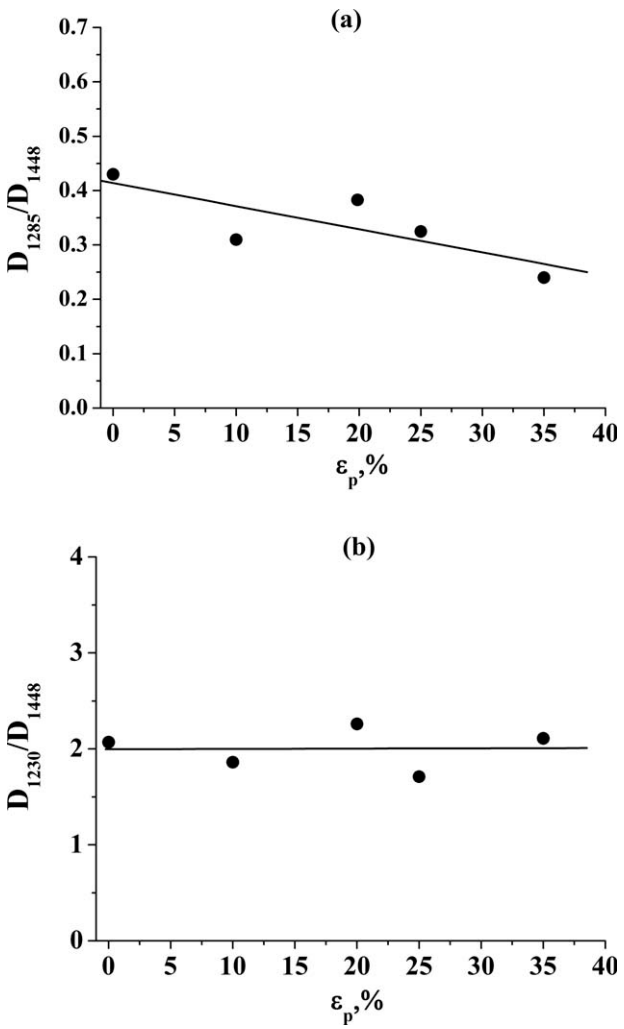

Figure 10 Change in the ratio of the absorbance of the bands at (a) 1285 and (b) 1230 cm^{-1} to that of the standard band during stretching.

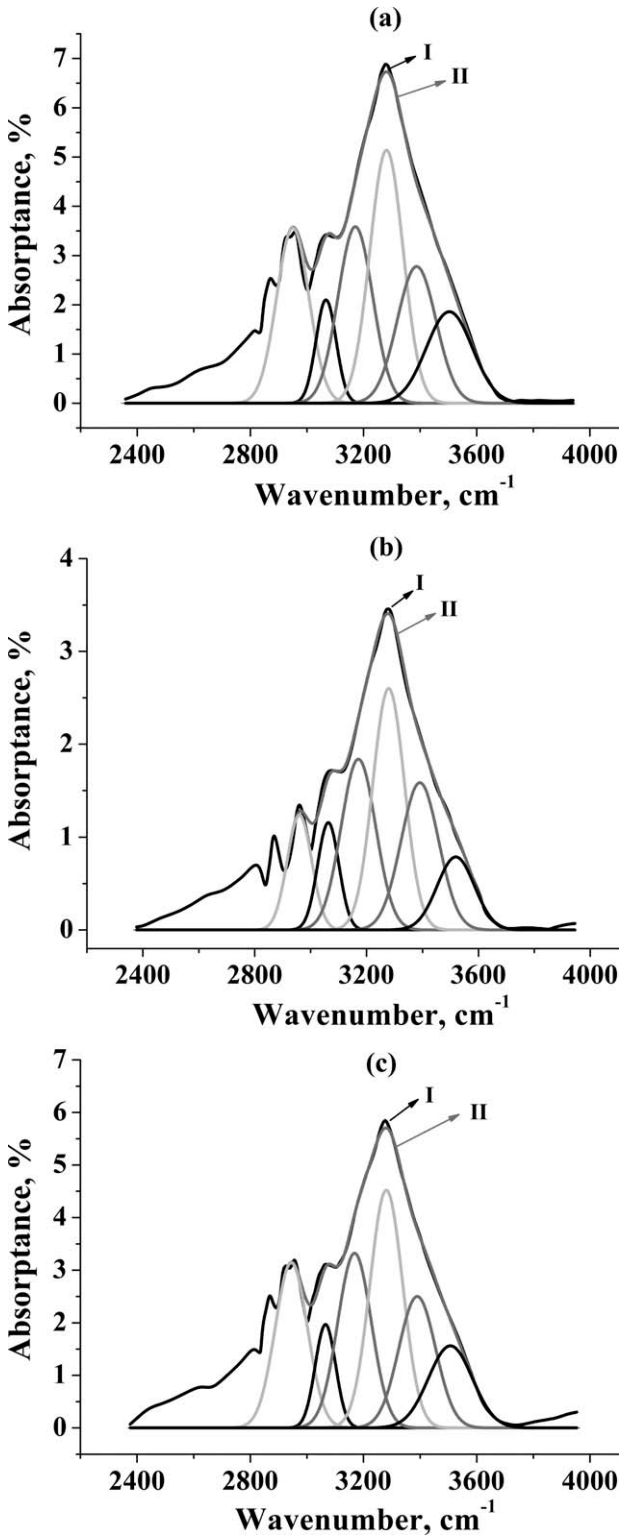

Figure 11 FTIR spectra in the 2400–4000-cm^{-1} region of wool fibers extended at different ε_p values: (a) 0, (b) 20, and (c) 35% resolved into components: (I) experimental spectrum and (II) curve fit.

molecules from the structure and the reorganization of hydrogen-bond interactions.

Also, to estimate the changes of disulfide (—SS—) groups that contributed to the physical and mechanical properties and the structural stability of the wool fiber, the spectral region of 600–1150 cm^{-1} for different pre-extension levels, shown in Figure 13, was examined. Here, the band at 1040 $cm^{-1,}$ assigned to sulfonate S—O stretching, was attributed to cysteic acid.[21,24,33] The ratio of the absorbance of this band did not change much for ε_p values up to around 25% and increased slightly for ε_p values greater than 25–30%, as shown in Figure 14. This result suggests that the some of the cystine S—S bonds producing —SH groups were broken, and by undergoing oxidation, some of —SH groups were converted to cysteic acids. The number of broken S—S bonds and the conversion of —SH groups to cysteic acid increased significantly for the extension levels falling in the postyield region.

Discussions

The mechanical tests revealed that the stretching of the wool fibers in the first Hookean deformation region ($\varepsilon_p < 4\%$) did not lead to significant changes in the mechanical characteristics (Figs. 2 and 4). This meant that the deformation in this region could be

TABLE III
Band Frequency and Half-Band Width of the Components in the 2400–3800-cm^{-1} Region of the FTIR Spectra of the Wool Fibers Extended at Different Strain Levels

ε_p (%)	Band frequency (cm^{-1})	Half-band width (cm^{-1})
0	2950	110
	3067	64
	3171	119
	3281	113
	3388	134
	3503	160
10	2940	110
	3064	70
	3170	118
	3277	108
	3382	126
	3503	151
20	2960	82
	3063	70
	3171	120
	3279	109
	3391	131
	3519	129
25	2943	100
	3065	68
	3171	115
	3280	111
	3388	130
	3503	157
35	2945	110
	3066	65
	3168	115
	3281	112
	3390	126
	3506	152

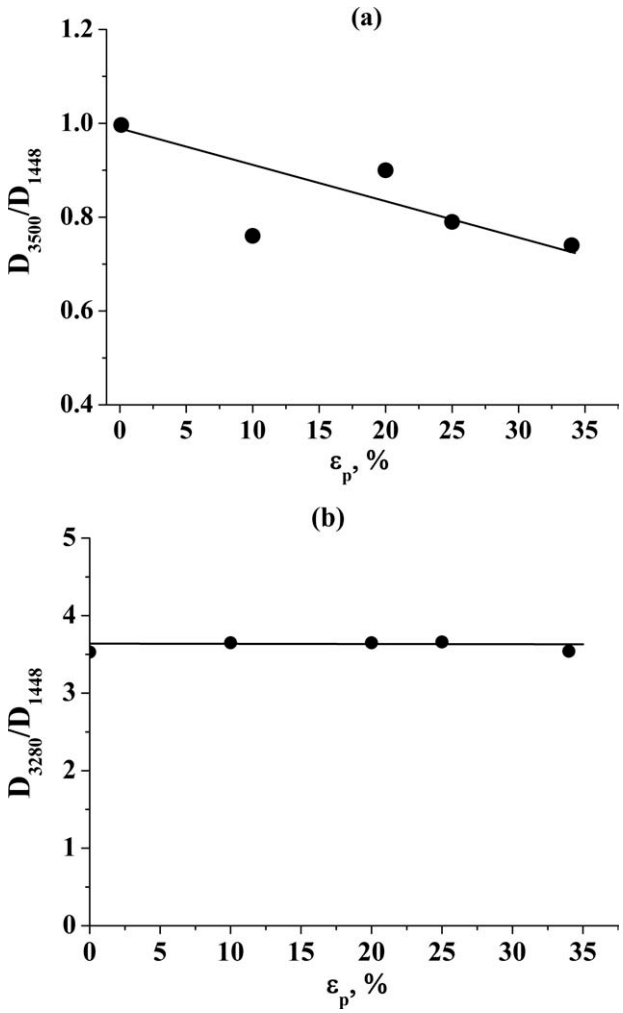

Figure 12 Change in the ratio of the absorbance of the bands at (a) 3500 and (b) 3280 cm^{-1} to that of the standard band during stretching.

attributed to elastic deformation in the structural elements of the fiber. Deformation beyond a 4% strain led to considerable changes in the mechanical properties, depending on the strain level (Figs. 2, 4, and 5); the only one quite stable characteristic was E_i. It is well known that the tensile properties of keratin fibers are mainly related to the α–β conformational transition in the microfibrils; this was also proven with our FTIR experimental results, both in the yield and postyield deformation regions [Figs. 8(a,b) and 10(a)]. Also, one very interesting structural feature was revealed from the FTIR spectral data; this was the presence of the stable β form, which was not sensitive to stretching [Figs. 8(c) and 10(b)]. We supposed that this rather stable structure could determine the stability of E_i of the stretched wool fibers. The decrease in the breaking extension with increasing ε_p (Fig. 4) could be explained by the occurrence of α–β conformational transitions. The higher the ε_p was, the more units of the microfibrils were transformed from α helices to extended

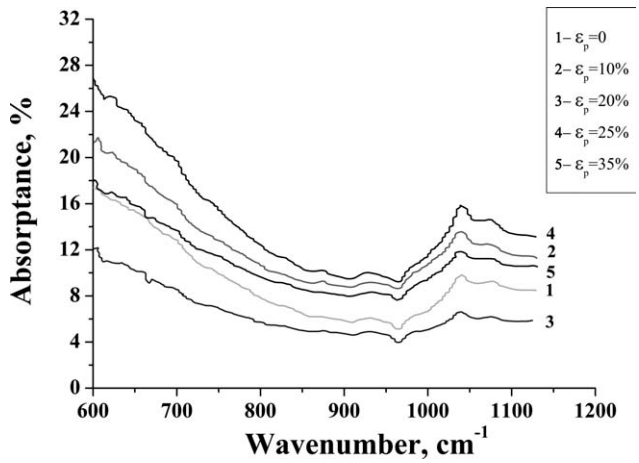

Figure 13 FTIR spectra in the 600–1150-cm^{-1} region of wool fibers extended at different ε_p values.

β sheets. Therefore, the second stretching of the pre-extended fiber came out thanks to the opening of fewer helical units, which were not opened in the first stretching.

Another important characteristic of stretched wool fibers is σ_r. Here, we have to remember that this characteristic is tightly coupled with the size of the fiber cross section; that is, the stress is inversely proportional to the size of the cross section. We showed that the diameter of the wool fibers decreased maximally by 10–12% after stretching (Fig. 3). The other process that could support the increase in the stress at break of the stretched wool fibers was the reorganization of intermolecular interactions between structural elements. The stretching of the wool fiber caused the breakage of the quite strong intramolecular hydrogen bonds in the helices and intermolecular hydrogen bonds between the microfibrils and matrix globules. However, why did the band with a maximum near 3280 cm^{-1} in the FTIR spectra of the

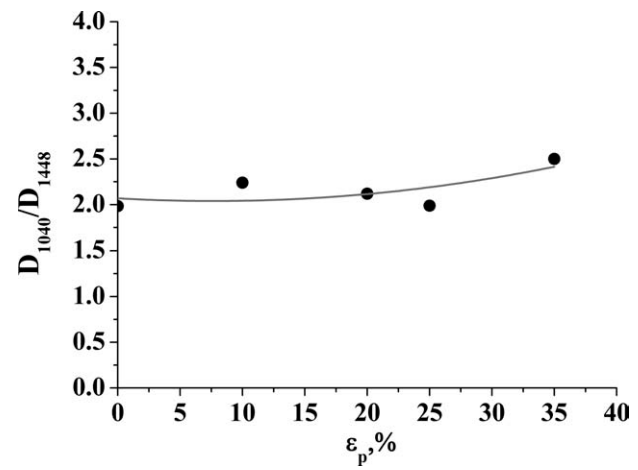

Figure 14 Change in the ratio of the absorbance of the band at 1040 cm^{-1} to that of the standard band during stretching.

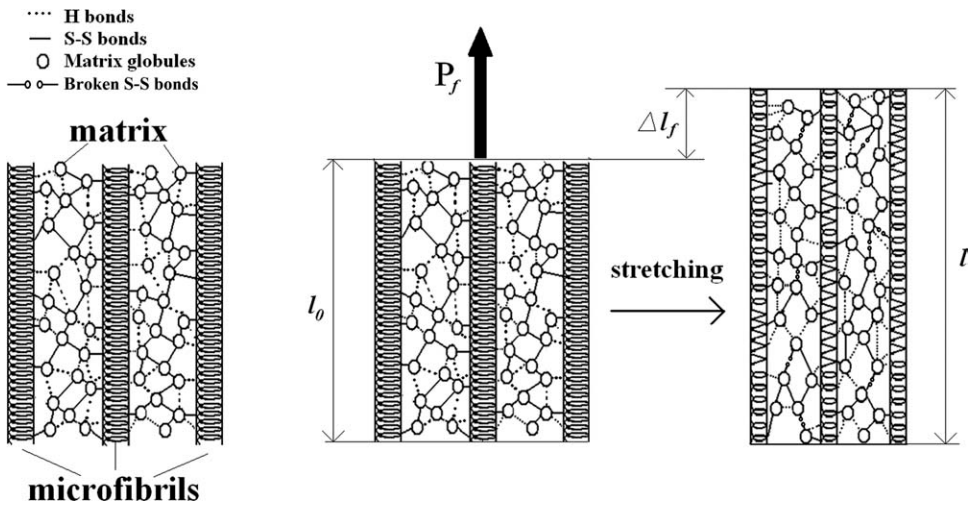

Figure 15 Structural model showing the deformation processes in the wool fiber. l_0, l, and Δl_f are the length of the unstretched fiber, the length of the stretched fiber, and the change in the length of the stretched and unstretched states of the fiber ($\Delta l_f = l - l_0$), respectively.

stretched wool fibers not change significantly? The following explanation is proposed. The orientation processes in the fiber occurred together with the approach of the structural elements to each other, which caused the removal of water molecules from the spaces in the matrix (Fig. 12). In the initial state, the matrix globules predominantly interacted with each other and the microfibrils by hydrogen bonds through water; this formed polymer–water–polymer bridges. The removal of water molecules caused the appearance of stronger types of hydrogen bonds, such as polymer–polymer bonds. These new hydrogen bonds were rather stable and fixed the new stretched form rather strong; this was proven by our previous investigation of the elastic recovery processes in wool fibers.[34] So, during stretching, we deal not only with the breakage of the strong type of hydrogen bonds between helices but with the reorganization of the hydrogen-bond network in the keratin structure of the wool fiber.

On the other hand, as shown in Figure 14, the absorbance of the S—O stretching band did not change much, as ε_p increased up to around 25%, and included the deformation in the yield region. This indicated that almost all of the broken disulfide groups, mostly located between matrix globules and connecting with some sides of the microfibrils, as shown in Figure 15, were reconnected; hence, the absorbance of the sulfonate S—O stretching band did not change significantly. This indicated an almost constant content of cysteic acids. However, ε_p values greater than 25–30%, which fell in the postyield region, led to an observable increase in the absorbance of S—O band. This indicated that more —SS— groups were broken, and although most of them were reconnected again, after oxidation some of the —SH groups were converted to cysteic acids. We can say that eventually, the number of broken disulfide bonds increased significantly for the ε_p's falling in the postyield region; this led to a decrease in the mechanical properties.

Moreover, we supposed that some of cysteic acids could return to cystine residues to form the disulfide bonds between globules in the matrix because of the interaction with water molecules because our previous work[34] showed that extended fibers (up to 40%) obtained a complete recovery of the mechanical properties and the original stress–strain curve after they were kept in water for a short time. We suggest that all the newly broken disulfide bonds (S—S) and newly formed cysteic acids were not stable under room conditions. However, the newly formed unstable cysteic acids could have been completely recoverable; that is, they could have formed disulfide crosslinks between the matrix globules when the stretched fibers interacted with water molecules; this implies a strong role of hydrogen bonds in the stretching and recovery processes of the wool fibers.

Another interesting result was the increase in E_y in the yield region after stretching, as shown in Figure 5. The figure depicts the slight increase in the modulus when ε_p ranged from 4 to 16% strain and a drastic increase beyond 16% strain. The increase in E_y could not be explained by only the α–β conformational transition in the microfibrils. Thus, we supposed an important contribution of the matrix to the change in the mechanical characteristics. If we were to suppose that the change in the stress–strain curve of the stretched fiber was related only to the α–β transition, we would see only the shortening of the yield region but not the increase of its slope. We explained the increase of the slope in the yield region by the orientation processes in matrix, which

occurred, as we mentioned previously, because of the reorganization of hydrogen bonds. This oriented form was held by a new, strong type of hydrogen bond. We supposed that the matrix phase had a netlike structure and, therefore, the following properties: a low value of the modulus in the beginning of stretching that increased during orientation. Such a netlike structure of the matrix was also proposed earlier from other experimental results.[34] Thus, we suppose that the curve in Figure 5 shows the modulus of the matrix phase changes from 0.07 to 1.6 GPa during stretching.

The structural model of the wool fiber, where microfibrils played the role of a reinforcing phase, and the matrix filler is illustrated in Figure 15. Here, in the sulfur-rich protein matrix, crosslinking disulfide bonds were mostly located between the matrix globules, and they also connected some globules with some microfibrils. Because the microfibrils had low-sulfur proteins,[1] there were some crosslinking disulfide bonds between the helices in the microfibrils, which are not shown in Figure 15. For such a composite system, where the components are connected in parallel, if we know the rigidity of the matrix, we can calculate the rigidity of the microfibrils. We can write the load (P_f) for such a system as follows by considering the stress and cross-sectional areas for each element:

$$\sigma_f A_f = \sigma_{mf} A_{mf} + \sigma_m A_m \tag{1}$$

where σ_f, σ_{mf}, and σ_m are the stresses in the fiber, the microfibrils, and the matrix, respectively, and A_f, A_{mf}, and A_m are the cross-sectional areas of the fiber, the microfibrils, and the matrix, respectively. Dividing both parts of eq. (1) by A_f, we get the relation:

$$\sigma_f = \sigma_{mf}\theta_{mf} + \sigma_m\theta_m \tag{2}$$

where θ_{mf} and θ_m are the contents of the microfibrils and the matrix in the fiber cross section, respectively, and are written as follows:

$$\theta_{mf} = \frac{A_{mf}}{A_f} \quad \text{and} \quad \theta_m = \frac{A_m}{A_f} \tag{3}$$

By using Hook's law, we obtain the following equation:

$$E_f\varepsilon_f = E_{mf}\varepsilon_{mf}\theta_{mf} + E_m\varepsilon_m\theta_m \tag{4}$$

where E_f, E_{mf}, and E_m are the initial rigidities of the fiber, the microfibrils, and the matrix, respectively. ε_f, ε_{mf}, and ε_m are the strain of the fiber, microfibrils, and matrix, respectively. Because the strain of each component is equal to that of the fiber, by removing strain terms from eq. (4), we can rewrite eq. (4) as follows:

$$E_f = E_{mf}\theta_{mf} + E_m\theta_m \tag{5}$$

Here, if we take the approximate values for the content of microfibrils and matrix and use the following assumptions, we can roughly estimate the contribution of the matrix and microfibrils. From different literature sources, it is known that the content of microfibrils in wool fiber is about 20–35%.[1,35] If we take an approximate value of 30% for θ_{mf}, θ_m becomes 70%. Thus, we can write the following relation for the estimation of E_{mf}:

$$E_{mf} = \frac{E_f}{0.3} - \frac{0.7E_m}{0.3} \tag{6}$$

As we have assumed from our experimental results, E_m increases from 0.07 to 1.6 GPa during stretching (Fig. 5). So we supposed that in the beginning of stretching, the matrix had a rigidity 0.07 GPa or lower. If the initial modulus of the fiber (E_f) was taken as 6 GPa, which was compatible with our experimental results, by using these data and eq. (6), we can obtain the approximate value of the modulus of the microfibrils (E_{mf}) as 19.85 GPa.

Consequently, from our experimental results, we supposed the following structural processes during the stretching of the wool fiber. The initial deformation of the fiber (deformation $< 4\%$) was determined predominantly by stiff microfibrils having a modulus of approximately 20 GPa. After overcoming the yield point estimated at approximately 4% strain, the rigidity of the microfibrils decreased rapidly because of the destruction of intrahelical hydrogen bonds that, in fact, determined its stiffness. Such a rapid destruction of hydrogen bonds occurred because the critical distance between the turns of the helices was overcome; this was needed for the appearance of hydrogen bonds. The subsequent stretching caused α–β conformational transition in the microfibrils and the orientation of the matrix along the stretching axis.

CONCLUSIONS

The mechanical characteristics and the conformational changes in wool fibers were examined, and the contribution of the microfibrils and the matrix to the deformation processes in the wool fibers were analyzed. The mechanical tests enabled us to roughly estimate the modulus of the matrix, which changed from 0.07 to 1.6 GPa during stretching and proved the proposal about the netlike structure of the matrix, which could be easily stretched up to high deformation values without irreversible

changes. Although the rupture of some cystine S—S bonds, some of which were converted to cysteic acids with oxidation, led to a slight decrease in the mechanical strength, the stretched state of the wool fiber was fixed by the great number of hydrogen bonds located between the matrix globules and the microfibrils, and among the matrix globules themselves, which contributed to the increases in the rigidity and strength of the stretched wool fiber.

On the basis of the experimental data and the structural model, where microfibrils play the role of the reinforcing phase and the matrix filler, the rigidity of the microfibrils in the initial unstretched state was estimated roughly as approximately 20 GPa; this has not been observed in the literature so far. The tensile tests of the stretched wool fibers revealed significant changes in the mechanical characteristics, except E_i, which retained a constant value. However, because all visible changes were related to the conformational transition, the reorganization of hydrogen-bond interactions, and the change of disulfide bonds, they could be completely recovered and were reversible, as shown in our previous study.[34] We supposed a crucial role of the matrix net, especially for the recovery processes, in the wool fiber.

References

1. Feughelman, M. J Appl Polym Sci 2002, 83, 489.
2. Hearle, J. W. Int J Biol Macromol 2000, 27, 123.
3. Wortmann, F. J.; Zahn, H. Text Res J 1994, 64, 737.
4. Feughelman, M. Text Res J 1959, 29, 223.
5. Wojciechowska, E.; Rom, M.; Wlochowicz, A.; Wysocki, M.; Weselucha-Birczynska, A. J Mol Struct 2004, 704, 315.
6. Pielesz, A.; Freeman, H. S.; Weselucha-Birczynska, A.; Wysocki, M.; Wlichowicz, A. J Mol Struct 2003, 651–653, 405.
7. Horton, H. R.; Moran, L. A.; Scrimgeour, K. G.; Perry, M. D.; Rawn, J. D. Principles of Biochemistry; Pearson: Parsippany, NJ, 2006; p 92.
8. Lehninger, A. L. Biochemistry; Worth: New York, 1972; p 111.
9. Feughelman, M. Text Res J 1994, 64, 236.
10. Chapman, B. M. Text Res J 1969, 39, 1102.
11. Crewther, W. G. Text Res J 1972, 42, 77.
12. Feughelman, M.; Haly, A. R. Biochim Biophys Acta 1959, 32, 596.
13. Liu, H.; Yu, W. J Appl Polym Sci 2007, 103, 1.
14. Taddei, P.; Monti, P.; Freddi, G.; Arai, T.; Tsukada, M. J Mol Struct 2003, 650, 105.
15. Tsobkallo, E. S.; Tiranov, V. G.; Gromova, E. S. Fibre Chem 2001, 33, 215.
16. Tsobkallo, E. S.; Chmel, A. E.; Tikhomirov, A. A. Fibre Chem 2006, 38, 41.
17. Tsobkallo, K.; Tikhomirov, A.; Tshmel, A. Polymer 2004, 45, 1689.
18. Lyman, D. J.; Wijelath, J. M.; Feughelman, M. Appl Spectrosc 2002, 55, 552.
19. Paquin, R.; Colomban, P. J Raman Spectrosc 2003, 38, 504.
20. Akhtar, W.; Edwards, H. G. M.; Farwell, D. W.; Nutbrown, M. Spectrochim Acta A 1997, 53, 1021.
21. Kuzuhara, A. Biopolymers 2007, 85, 274.
22. Church, S.; Corino, G. L.; Woodhead, A. L. Biopolymers 1997, 42, 7.
23. Manas, E. S.; Getahun, Z.; Wright, W. W.; Degrado, W. F.; Vanderkooi, J. M. J Am Chem Soc 2000, 122, 9883.
24. Kuzuhara, A.; Horri, T. Biopolymers 2005, 79, 173.
25. Mayo, D. W.; Miller, F. A.; Hannah, R. W. Course Notes on the Interpretation of Infrared and Raman Spectra; Wiley: Hoboken, NJ, 2003; Chapters 3 and 6.
26. Banwell, C. N. Fundamentals of Molecular Spectroscopy, 3rd ed.; McGraw-Hill: Maidenhead, United Kingdom, 1983; p 94.
27. Iwamoto, R.; Murase, H. J Polym Sci Phys 2003, 41, 1722.
28. Dechant, J. Ultrarotspektroskopische Untersuchungen an Polymeren; Akademie-Verlag: Berlin, 1972; p 322.
29. Bendit, E. G. Nature 1962, 193, 236.
30. Bilinska, B. Spectrochem Acta A 2001, 57, 2525.
31. Skrovanek, D. J.; Howe, S. E.; Painter, P. C.; Coleman, M. M. Macromolecules 1985, 18, 1676.
32. Wojciechowska, E.; Wlochowicz, A.; Weselucha-Birczynska, A. J Mol Struct 1999, 511–512, 307.
33. Alexandaer, P.; Hudson, R. F.; Earland, C. Wool: Its Chemistry and Physics, 2nd ed.; Chapman & Hall: London, 1963; p 268.
34. Tsobkallo, E.; Aksakal, B.; Darvish, D. J Macromol Sci Phys 2010, 49, 495.
35. Cao, J.; Billows, C. A. Polym Int 1999, 48, 1027.